UNIVERSITY OF CALIFORNIA, SAN DIEGO

Photomechanical actuation in RET-CNT composites

A thesis submitted in partial satisfaction of the requirements
for the degree Master of Science

in

Engineering Sciences (Mechanical Engineering)

by

Abhishek Golgod Sathisha

Committee in charge:

Professor Prabhakar R. Bandaru, Chair
Professor Shengqiang Cai
Professor Olivia Graeve

2017

The thesis of Abhishek Golgod Sathisha is approved and acceptable in quality and form for publication on microfilm and electronically:

Chair

University of California, San Diego

2017

TABLE OF CONTENTS

LIST OF FIGURES

LIST OF TABLES

ACKNOWLEDGEMENTS

I express a deep sense of gratitude to my advisor Dr. Prabhakar R. Bandaru, for providing me support and advice in times of need and without whose constant guidance and suggestion I would not be able to complete this degree. It is a great honor to be a part of his innovative team which has done phenomenal work in the field of material science.

I would like to thank Dr. Shengqiang Cai and Dr. Olivia Graeve for giving their valuable time to serve in my thesis committee.

I would like to thank Dr. Shengqiang Cai for providing me with clear insights to the problem and allowing to use the equipment in his lab.

A special note of thanks is due to all my co-workers: Zichen Zhang and Xudong Liang in helping me conducted the tests and complete the analysis; Dr. Krishna Vemuri for helping me through the initial stages of my research; Wei Fan for helping me comprehend the experimental setup at Dr. Cai's lab and also the others members of Dr. Bandaru's research group: Dr. Rajaram Narayanan, Darren Helstowski, Serdar Yavuz, Anna Alexander, Peng Chen, Bei Fan and Fatih Canbazoglu for supporting me through this research. I would also like to acknowledge Dr. Sunghoon Park for allowing me to use the SEM image of RET-CNT composite in my thesis.

I would also like to thank my friends: Amruth Bhargav, Harikrishnan Murali, Anudeep Padmanabhan, Vinod Kumar and Anay Pandit for editing the thesis and their constant support through the coursework.

Finally, I would like to extend my gratitude to my parents, without whom I would not be who I am today.

Chapter 3, in part, has been submitted for publication of the material as it may appear in. "Light induced reversible and irreversible deformation in nanotube-polymer

composites”, 2017, X Liang, Z Zhang, A Sathisha, S Cai, P Bandaru, Polymer, 2017. The thesis author was the co-author of this paper.

Chapter 4, in part, has been submitted for publication of the material as it may appear in. “Light induced reversible and irreversible deformation in nanotube-polymer composites”, 2017, X Liang, Z Zhang, A Sathisha, S Cai, P Bandaru, Polymer, 2017. The thesis author was the co-author of this paper.

Chapter 5, in part, has been submitted for publication of the material as it may appear in. “Light induced reversible and irreversible deformation in nanotube-polymer composites”, 2017, X Liang, Z Zhang, A Sathisha, S Cai, P Bandaru, Polymer, 2017. The thesis author was the co-author of this paper.

ABSTRACT OF THE THESIS

Photomechanical actuation in RET-CNT composites

by

Abhishek Golgod Sathisha

Master of Science in Engineering Science (Mechanical Engineering)

University of California, San Diego, 2017

Professor Prabhakar R. Bandaru, Chair

Carbon nanotubes (CNT) have been in the forefront of nanotechnology research since their discovery in 1991. Its multifunctional properties are used in diverse applications such as transistors, gaseous storage material and actuator to name a few. In this thesis, actuation in a composite of CNT with Reactive ethylene terpolymer (RET) due to light has been studied and compared with that observed in PDMS-CNT composite. While PDMS-CNT composite shows a reversible stress response under strain and incident light, RET-CNT yields a reversible stress response along with an irreversible stress response not observed in PDMS-CNT composite. Furthermore, the effects of parameters such as light intensity and uniaxial tensile strain have on actuation have been observed through accurate stress response measurements. Assuming melted crystalline domains of RET

as the cause of actuation in the composite, change in shear modulus as a function of number density of crystalline domains is calculated. Based on the results, a microscopic model for photomechanical actuation in thermoplastic-CNT composites is discussed.

1. INTRODUCTION

Carbon is one of the most abundantly available elements on earth. It is one of the building blocks of all forms of life. Commercially, carbon is essential to modern civilization through its multitude of applications such as a power source in the form of coal and hydrocarbons, a raw material for essential components like steel, polymers etc. to name a few. Carbon exists in the form of different allotropes such as graphite, diamond etc. Each allotrope differs from another in their physical properties. Depending on the application, different allotropes of carbon utilized as applicable. In the field of research, the recently discovered allotropes such as fullerenes, graphene, and nanotubes are being studied extensively due to their interesting physical properties.

The discovery of carbon nanotubes (CNT) by S.Ijima [1] in 1991 initiated intense research interest in them. The research over a decade infers that CNT exhibit rare amalgamation of mechanical strength, stiffness and low density with exceptional transport properties. These attributes have made CNT an ideal choice for multifunctional materials that combine the best of CNTs with other materials such as polymers, ceramics, and metals [2], [3]. Thus, CNTs are blended with other materials to obtain tailored materials for various applications such as transistors, as hydrogen storing material, as probes and sensors [3]; in lightweight bicycles, antifouling coating of ship hulls, electrostatic discharge shield on satellites [4], artificial muscles [5], [6] and actuators [7]–[9] etc.

Actuators are utilized in a wide variety of actuation application in various fields such as robotics, artificial muscles, micro-electro-mechanical-systems and micro-opto-mechanical-system. It is achieved by converting different types of energy to mechanical energy to move or control a mechanism or a system. On a macroscopic scale, actuators

can be powered using materials such as piezoelectric materials [10], conducting polymers [5], [8], shape memory alloys etc. The process is quite efficient as well. However, on a micro- and nanoscale, such materials are not suitable. Critical issues such as scalability into nanoscales, high performance and ease of operation for implementation in nanotechnology and biomedical impedes their applications severely. Under such circumstances, substitutes such as metallic nanoparticles, nanowires, and CNTs could be used instead. Nanotubes and nanowires have been used to configure dynamic systems like cantilever beams, linear and torsional actuators on a nanoscale level in laboratory conditions. Nanostructures, particularly those made of CNT, exhibit actuation to applied external stimuli such as heat, electric voltage, and light.

The aim of this dissertation is to investigate the photomechanical properties of the CNT-based composite. To this end, the dissertation is structured as follows:

Chapter 2 discusses the general background of carbon nanotubes and Reactive Ethylene Terpolymer (RET), the polymer matrix. Chapter 3 explores the process of fabrication of the composite in a detailed manner. Chapter 4 discussed the experiments conducted to investigate the photomechanical actuation and discuss the results of the experiment. Chapter 5 suggests a mechanism describing the photomechanical actuation process. Chapter 6 concludes the dissertation with a summary of the study.

2. BACKGROUND

With a combination of outstanding mechanical, electrical, thermal and optical properties, CNTs are considered elementary to nanotechnology. A better understanding of these properties is critical to manipulating CNTs to obtain customized novel materials for specific applications. A lot of research efforts has been done to understand the interplay between the properties of CNT. In this direction, this section provides a brief review of basic structure and properties of CNTs. Additionally, this section also provides a review of the RET, which is extensively used in this study.

2.1 FUNDAMENTALS OF CARBON NANOTUBE

Since the discovery of multi-walled carbon nanotube (MWCNT), the researchers were stimulated by the possibility of one-dimensional quantum effects due to their electronic properties [11] and promising mechanical properties. Experimental characterization of a more fundamental single-walled carbon nanotube (SWCNT)

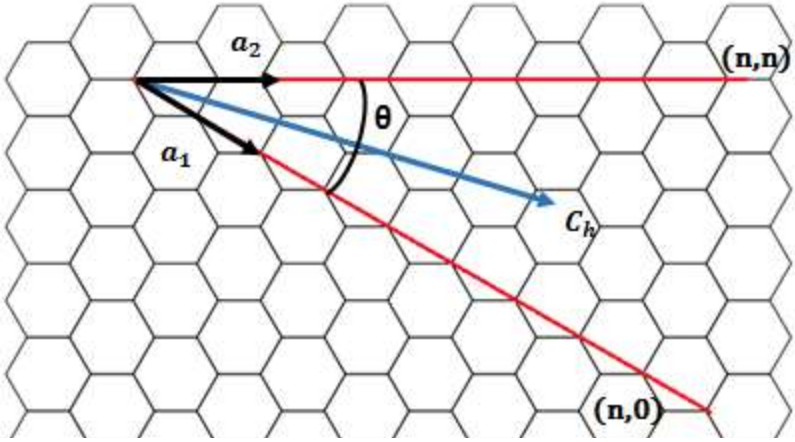

Figure 1: Schematic representation of 2D graphene sheet with basis and chiral vectors. The lines (n,n) and (n,0) represent the armchair and zigzag configurations

independently in 1993 by Iijima [12] and Bethune [13] further motivated researchers. The discovery of SWCNT led to many remarkable breakthroughs such as hydrogen storage[3], nanoelectrodes [14], and supercapacitor electrodes[15].

An ideal SWCNT is a long cylindrical tubule capped with hemispherical structures, which when combined form a fullerene [3], [16]. The cylindrical portion of SWCNT is made of a single rolled up graphene sheet. CNT tubules can be conveniently specified with tube diameter 'd' and chiral angle 'θ' as shown in figure 1. The chiral vector $\mathbf{C_h}$ can be defined using integers *(n,m)* and basis vectors $\mathbf{a_1}$ and $\mathbf{a_2}$ as

$$\boldsymbol{C_h} = n\boldsymbol{a_1} + m\boldsymbol{a_2} \quad (1)$$

where integers *n* and *m* can be used to obtain diameter *d* and chiral angle θ, with respect to zigzag axis using the formulations in Table 1.

Table 1: Formulations to calculate diameter d and chiral angle

Symbol	Name	Formula
d	Diameter	$d = \frac{a\sqrt{n^2 + m^2 + nm}}{\pi}$
θ	Chiral angle	$sin\theta = \frac{\sqrt{3}m}{2\sqrt{n^2 + m^2 + nm}}$
		$cos\theta = \frac{2n + m}{2\sqrt{n^2 + m^2 + nm}}$
		$tan\theta = \frac{\sqrt{3}m}{2n + m}$

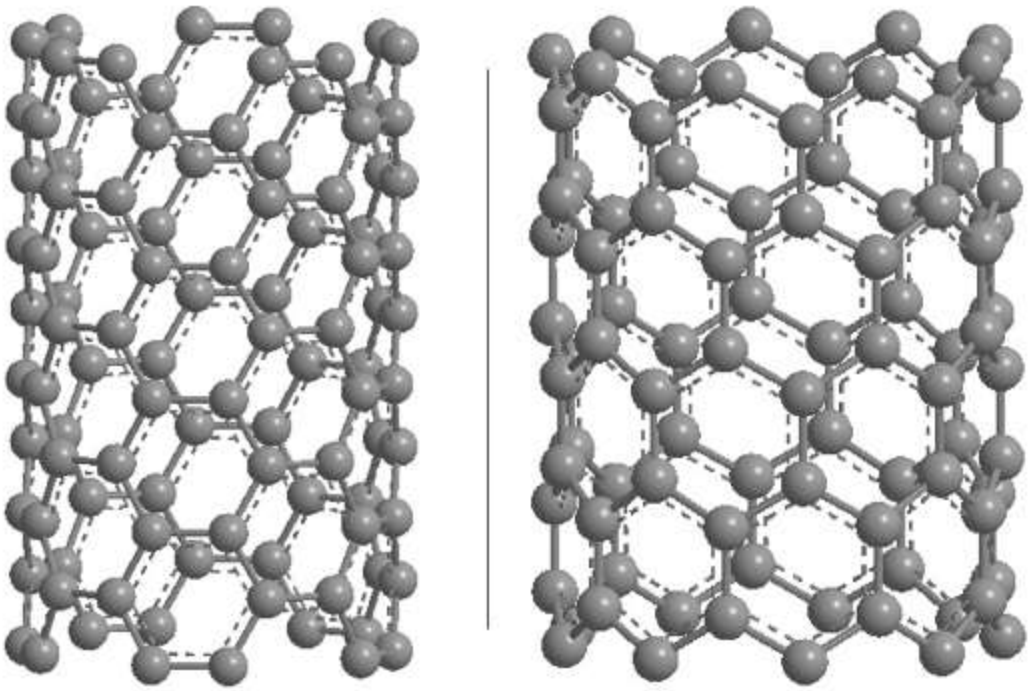

Figure 2: 3D representation of armchair and zigzag configuration of CNT

Based on the chiral angle, CNT structure can be divided into 3 types; 1) zigzag, where θ = 0°, 2) armchair, where θ = 30°, 3) chiral, where 0° < θ < 30°. The integers *(n, m)* determine whether CNT would behave as a metal or a semiconductor. Zigzag structures, i.e. *(n, 0)* has two distinct behaviors: as a metal when n/3 is an integer and semiconductor otherwise. Chiral structures, much like zigzag, behave as metals when (2n+m)/3 is an integer and as a semiconductor otherwise. Armchair structures i.e. *(n, n)* behave like a true metal [16]. The ability of SWCNT to behave as a metal or a semiconductor, depending on its geometric parameters such as chiral angle and diameter has resulted in SWCNT-made field effect transistors.

MWCNT structure is slightly different from that of SWCNT. Instead of just one nanotube, the structure of MWCNT consists of multiple tubules nested within each other. The outer diameter is usually in the range of 20 to 30 nm depending on the number of walls within a nanotube. The electronic properties of the MWCNT depend on the

outermost tubule resulting in either a metallic or semiconductor-like behavior depending on the chirality of the outermost tubule.

Since its discovery, CNT was expected to have superlative mechanical properties comparable to that of graphene. Computational simulations conducted by *Overney et al.* also provided similar results predicting Young's modulus to be 1500 GPa [17], [18]. The first mechanical tests were conducted on MWCNT in 1997 by *Wong et al* using atomic force microscope (AFM) which yielded Young's modulus of 1.28 TPa and average bending strength of 14 GPa [18], [19]. However, generally accepted value Young's modulus was measured by *Yu et al.* in 2000 obtained through measuring stress-strain measurements of an MWCNT pinned at one end inside an electron microscope. Young's modulus was measured between 270 – 950 GPa. The outermost layer of MWCNT failed at applied tensile loads ranging between 11 and 63 GPa at strains up to 12% ("sword-in-sheath" failure). Using the same method, *Yu et al.* could measure Young's modulus for SWNT to be in the range 370 – 1470 TPa and tensile strength to be between 10 and 52 GPa. The toughness of SWCNT was estimated to be 770 J/g and MWCNT to be 1270 J/g [18], [20].

As a carbon allotrope, CNT like diamond and graphite is a very good conductor of heat. However, due to technological shortcomings associated with experimental measurements on a nanoscale, the direct and quantitative measurements of thermal conductivity of CNT individually is yet to be achieved. Hence, the thermal conductivities obtained so far has been due to experiments and computational simulations with significantly scattered results ranging between 2000 and 6000 W/m-K [18]. The thermal conductivity depends on the atomic arrangement, geometric parameters such as diameter and length of the tube, structural defects on the surface of the CNT and impurities within them. Transport of thermal energy within the CNT is assumed to occur through phonon

conduction mechanism, a mechanism common amongst non-metallic materials. The phonon conduction mechanism is influenced by parameters such as number of phonon active nodes, boundary surface scattering, the length of the free mean path for the phonons and inelastic Umklapp scattering [18], [21].

2.2 INTRODUCTION TO REACTIVE ETHYLENE TERPOLYMER

For this study, MWCNT is dispersed in a polymer matrix of Reactive Ethylene Terpolymer to study photomechanical actuation. RET (marketed by DuPont™ as Elvaloy® 4170, density 0.94 g/cm^3) is composed of 3 monomers namely, polyethylene, a methyl-methacrylate group, and epoxide group. Polyethylene and methyl-methacrylate groups contribute elastomeric properties and corrosion resistance. Ethylene group helps in physical cross-linking by forming crystalline domains [22], [23]. The two groups are vital for hot melt adhesive and coating applications. In the presence of CNTs with functional groups such as -OH, -COOH etc. the epoxide group forms ring bonds and provides

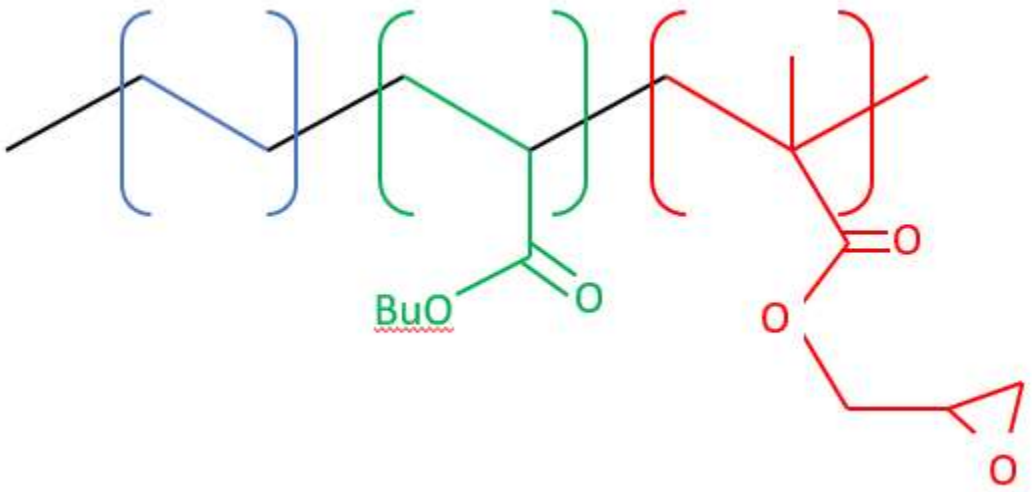

Figure 3: Chemical structure of RET. RET consists of three functional groups: ethylene (blue), butyl (green) and epoxide (red)

anchoring. The physical properties of RET are provided in table 2 and the physical structure is depicted in figure 3.

Table 2: Physical and thermal characteristics of RET

Density	0.94 g/cm^3
Young's Modulus	5 MPa
Tensile strength	4.5 MPa
Elongation at break	526%
Melting temperature	29.5 - 87°C
Glass transition temperature	-39.8°C
Melt flow index	8 g/10 min

3. FABRICATION AND EXPERIMENTAL SETUP

3.1 DISPERSION OF CNT

One of the important features of CNT is its large aspect ratio (generally >1000). However, the large aspect ratio of CNT possesses the disadvantage of entanglements and consequently form agglomerates. The presence of CNT agglomerates in composites would reduce its stiffening ability. The rate of agglomeration depends on inter-tube van Der Waal's (VDW) attraction, which is anomalously high in case of CNT due to its high polarizability. The agglomerates can be disentangled with the use of surfactants (to overcome VDW attraction amongst the CNT) and shear stress to disperse them. However, in certain occasions, surfactants are not used to preserve the highly electronically active surface of CNT. Sometimes, a stabilizing agent is used to stabilize the dispersed CNT within the matrix [24], [25].

Shear stress can be applied through varies means such as ultrasonication, shear mixing etc. In this study, ultrasonication is used to apply shear stress

3.2 ULTRASONICATION

Ultrasonication is a process of dispersion where the particles in a solution are agitated with ultrasonic sound energy. It is one of the most frequently used methods for particle dispersion. It is achieved using either an ultrasonic horn/probe or ultrasonic bath (Figure 4). The sonic energy imparted is dependent on ultrasound frequency and intensity, pulse interval, the concentration of solute, external pressure and temperature and in the case of an ultrasonic bath, container geometry [25].

Figure 4: Ultrasonication bath and ultrasonication probe

At the core, both ultrasonic bath and probe work similarly, by the sequence of bubble nucleation and collapse. The ultrasonic bath contains, usually, a rectangular bath where the solution to be dispersed is kept in a water bath. The ultrasonic energy is transmitted through water across the walls of the bath which affects the solution uniformly. Water should be maintained at the same level as the solution. In probe sonication, the probe, oscillating at a controlled frequency, is dipped in the solution to impart sonic energy. The oscillation of the probe tip initiates the formation of bubbles which results in cavitation due to its implosion, providing the energy for dispersion. An inert metal such as titanium is usually used to manufacture the probe. The tip of the probe is usually given a small taper to focus its intensity [26].

Sonication takes place because of bubble nucleation and collapse. This process is called acoustic cavitation [27]. The rapidly oscillating bath/probe tip produces a field of high energy, resulting in bubble formation. The bubble, thus formed, separates the entangled CNTs as the bubble grows. When the bubble implodes, the energy released causes dispersion. On certain instances, the energy released is high enough to fragment

CNT. During implosion, the time (~10^{-7} s) is just sufficient for the solution to diffuse into the opened gap within the boundary of the bubble [25]. The repeated cavitation process, along the length of the CNTs, helps the solution to penetrate and percolate between the tubes. Between the bath and probe, probe produces more defined cavitation zone and hence produces more localized energy than the bath [26].

A noteworthy observation is that the size of the bubbles thus produced is inversely proportional to the frequency of ultrasound. Likewise, the energy released is higher in the case of the implosion of larger bubbles formed due to lower frequencies (~20kHz) [24]. Hence, as the frequency is increased, nucleation and cavitation diminishes. It ceases altogether at frequencies higher than 2.5 MHz.

While the cavitation process is underway, a tensile stress is exerted on the CNT along its axis. The exerted tensile stress is of the order~70GPa which is high enough to break most CNTs. As the CNT breaks apart and its length decreases, the surface area over which the tensile stress is acting decreases. When the length decreases below a characteristic threshold L_{lim} the tubes scission ceases altogether. L_{lim} can be obtained by the following equation

$$L_{lim} = \sqrt{\frac{d^2\sigma}{2\eta\left(\dot{R}/_R\right)}} \quad (2)$$

Where d is the diameter of the CNT, σ is the tensile stress, η is the viscosity of the medium and R is the radius of the bubble.

Due to the violent cavitation, bubble formation can result in unwanted tube cutting, wall rupturing of the tube, resulting indenting, lattice modifications and reduction in a

number of layers in case of MWCNTs. Such localized damage causes deterioration of the electronic and mechanical properties of the CNTs.

3.3 EXPERIMENTAL PROCEDURE

The studied nanocomposite was fabricated using MWCNT obtained from Sigma-Aldrich Inc. and RET from DuPont™. MWCNT with an average diameter of 140nm, length ranging from 5 to 9 μm and density 2.1 g/cm^3 have been used.

Composite was prepared by dissolving pellets of RET in toluene. To speed up the process of the dissolution, the mixture was heated to 60°C for 2 hours. CNTs were sonicated for 10 minutes at 40% amplitude using a tapered probe type sonicator (VCX-750, Sonic Materials Inc., 750 W, 42 kHz) in toluene to disentangle from the agglomerates in preparation for better dispersion within the polymer matrix. The two mixtures were combined and sonicated at same settings for 1 hour to obtain a well-dispersed solution. The solution was stirred using a magnetic stirrer for 2 hours at 400 RPM and placed in a vacuum oven at 50°C for about 10 hours to obtain a jet black colored specimen. A scanning electron microscopy (SEM) image of the composite is shown in figure 5 to verify the uniform distribution of CNTs.

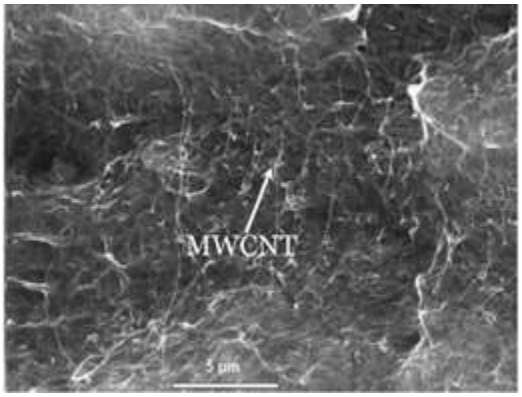

Figure 5: SEM image of a well dispersed RET-CNT composite (Photo credit: Dr. Sunghoon Park)

The well-dispersed RET-MWCNT composite is cut into pieces of dimensions, 25 *mm* × 5 *mm* × 0.3 *mm*. The samples are firmly clamped in between the grippers of the testing machine (5965 Dual Column Testing systems, Instron) and subjected to uniaxial tensile stress. During the test, both stress applied and the corresponding strain is automatically recorded by the machine and stress-strain diagrams for the composite are plotted. The strain was measured with an accuracy of ±0.1%. The sample was irradiated with a LED light source (CREE XM-L2 LED) positioned at 0.15m ± 0.01m away from the sample while tensile stress was applied. The light intensity was modulated in the range of 0 and 97 mW/cm^2 using neutral density filter manufactured by Thor Labs Inc.

For this study, composite with varied CNT content were fabricated, although, composites with 7wt% CNT were extensively used for tests. Any composite with CNT content more than the percolation threshold (~ 2.3wt%) was comprised of connected MWCNTs

Figure 6: Instron 5965 Dual Column Testing Solutions (Photo credits: Instron Inc.)

Chapter 3, in part, has been submitted for publication of the material as it may appear in. “Light induced reversible and irreversible deformation in nanotube-polymer composites”, 2017, X Liang, Z Zhang, A Sathisha, S Cai, P Bandaru, Polymer, 2017. The thesis author was the co-author of this paper.

4. TESTS AND RESULTS

In this section, we discuss the various tests conducted to determine the mechanism of photomechanical actuation.

The specimen was firmly held between the grips and irradiated with light and subjected to a uniaxial tensile strain to obtain actuation. Figure 7 represents the photomechanical actuation of RET-MWCNT composite with 7wt% CNT in the form of stress-time graph plotted at a constant strain of 50%. The light intensity was maintained at 97 mW/cm^2. The specimen was stretched and held at a pre-determined strain and allowed to relax into a quasi-equilibrium state from t = 0s to t = 1000s. Subsequently, the specimen was subjected to two intervals of light irradiation: 300s of light irradiation followed by another 180s of light irradiation with 300s of no incident light irradiation in between. After the light source was switched of applied tensile strain was removed at

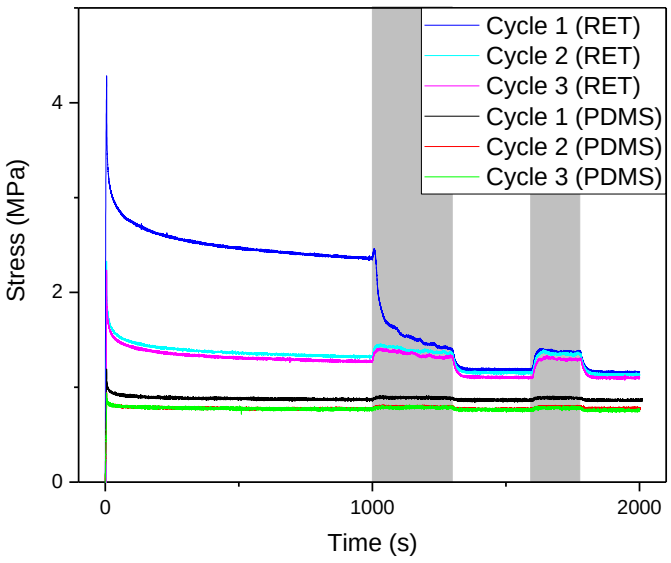

Figure 7: Stress response of RET-CNT and PDMS-CNT composites for 97mW/cm^2 light intensity and 50% applied strain

t = 2000s and allowed to contract in the free state. In the graph, time intervals marked in grey show the period of incident irradiation. This defines one entire cycle of photomechanical actuation in the testing.

A typical sample was subjected to three such cycles during the testing with 1000s seconds of a state of no stress and light irradiation between each cycle. When the specimen was irradiated with light for the first time in the first cycle (at t = 1000s), there was a slight increase in stress followed by significant stress relaxation till the light irradiation was stopped. The stress decreased further and stabilized when the light was switched off at t = 1300s. When the light was irradiated for the second time (at t = 1600 s) during cycle 1, the stress increased and maintained a stable value. Upon switching off the light source (at t = 1780 s), stress decreased to a value equivalent to that before the second irradiation. Substantial plastic deformation due to irreversible stress response was observed at the end of cycle 1. When the specimen was irradiated in cycle 2 and 3, stress increased and attained a stable value and upon switching off the light source and stress decreased to a value equivalent to that before the second irradiation upon switching the light source off. The first kind of stress relaxation is termed as ‘irreversible’ due to its non-repeatable nature and plastic deformation caused during the response. The second kind of stress response is termed as ‘reversible’.

The above tests were conducted for different concentration CNTs with RET as the polymer matrix a similar test conditions. The results obtained were similar to RET-CNT stress response curve shown in figure 7 with the presence of irreversible and reversible stress responses.

When PDMS-MWCNT composite was subjected to aforementioned procedure only reversible responses were observed. Figure 7 shows the stress-time graph of PDMS-

MWCNT stress response. *S.V. Ahir et al.* hypothesize that the photomechanical actuation is due to the *buckling or kinking of the CNTs* caused by polaron excitation in the PDMS-MWCNT composite [28]. Light is reported to be the main cause for actuation, which is further amplified by applied uniaxial tensile strain. The direction of extension (i.e. whether the sample will extend or contract) is dependent on applied uniaxial tensile strain. If the tensile strain is above a certain threshold (~ 10%), the specimen would extend and the specimen would contract when below the threshold.

RET, being a thermoplastic, behaves differently compared to PDMS. Our research group hypothesized that the ethylene segment in the RET forms crystalline domain serving as physical crosslinks. CNT dispersed in the matrix would convert irradiated light into heat, high enough to melt the crystalline domain. The melted domains would recrystallize with the removal of light. Since RET melts in the range between 29.5°C and 87°C [29], melting of crystalline domains could be the reason for the irreversible stress-response.

From the initial tests, it was evident that the cause for actuation was irradiated light and tensile strain. Tests were conducted to study the effects of these parameters by varying one parameter at a time keeping the other constant. The effects of uniaxial tensile strain on RET-MWCNT composite were studied by keeping the light intensity and CNT concentration at 97 mW/cm^2 and 7 wt% respectively. The tensile strain was varied using a computer controlled transducer cell of the testing machine. The testing procedure was similar to the process described earlier. Stress-time graphs of tests with uniaxial tensile strain 5%, 10%, 20%, 30% and 50% of specimen length are shown figure 8, 9, 10, 11, and 12 respectively. The graphs depict an increase in the magnitude of irreversible and reversible stress response with the increase in applied tensile strain. The magnitude of the stress response could be modulated by varying applied tensile strain. Interestingly,

when the graphs were normalized with the respective stress response recorded at the beginning of the light irradiation at t = 1000s, the curves collapse on top of each other (figure 13). This showed that stress response was *amplified proportionally with respect to uniaxial stress-strain*. A similar phenomenon was observed when cycle 2 and 3 stress responses were normalized as shown in figure 14 and 15. In PDMS-CNT, a similar stress response, but without irreversible response has been reported [28]. Irrespective of the polymer matrix, both systems depend on light intensity to exhibit actuation.

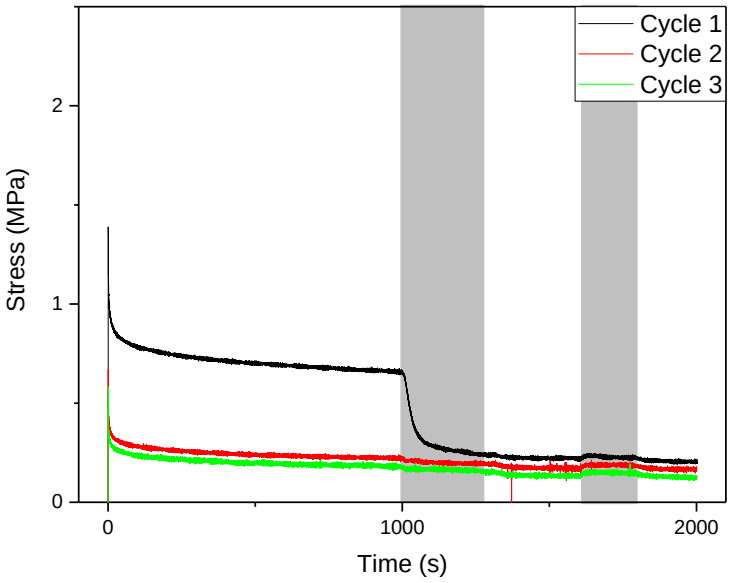

Figure 8: Stress response of RET-CNT composite for 97mW/cm^2 light intensity and 5% applied strain

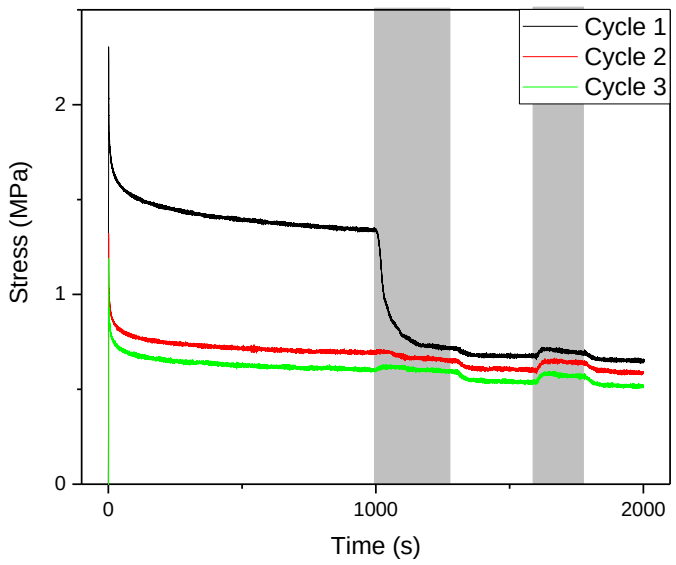

Figure 9: Stress response of RET-CNT composite for 97mW/cm^2 light intensity and 10% applied strain

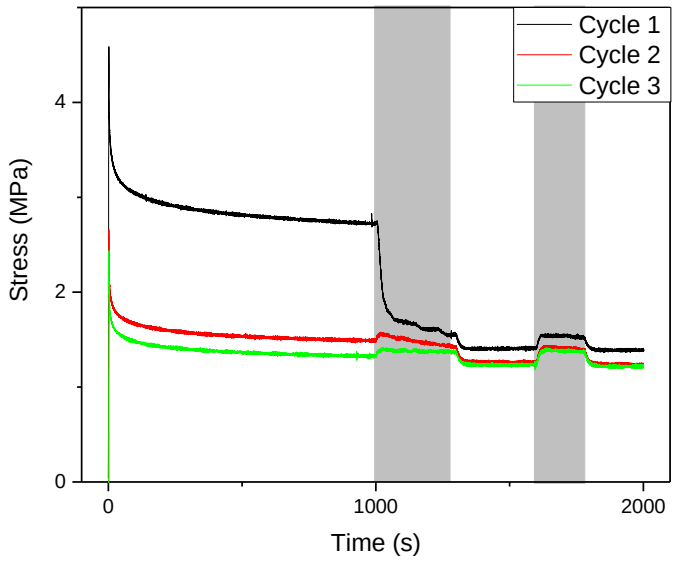

Figure 10: Stress response of RET-CNT composite for 97mW/cm^2 light intensity and 20% applied strain

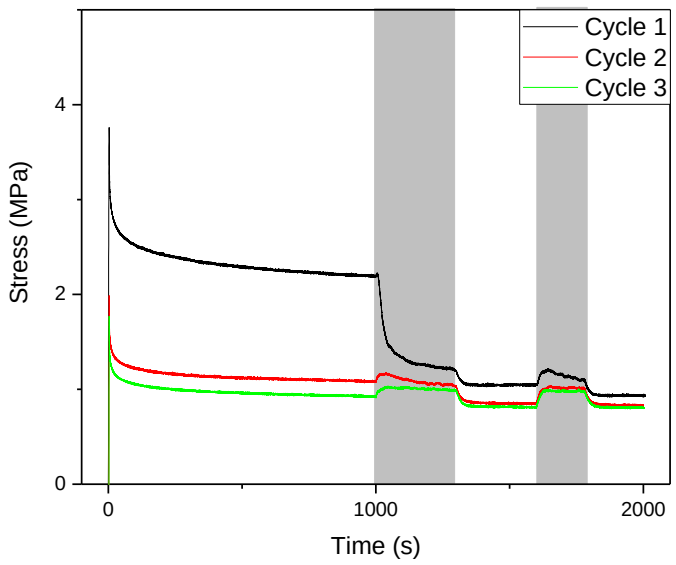

Figure 11: Stress response of RET-CNT composite for 97mW/cm^2 light intensity and 30% applied strain

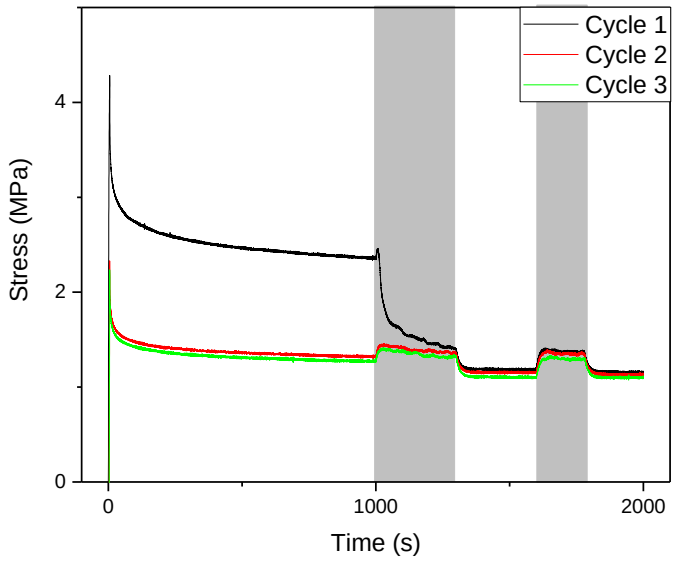

Figure 12: Stress response of RET-CNT composite for 97mW/cm^2 light intensity and 50% applied strain

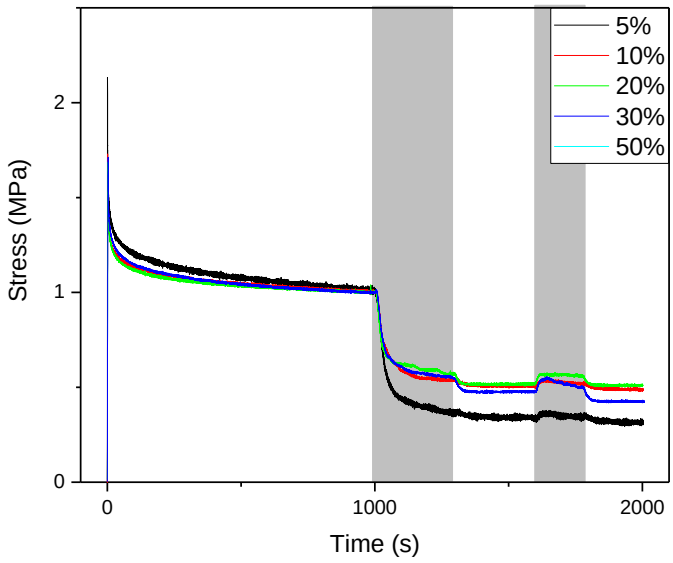

Figure 13: Normalized stress response of cycle 1

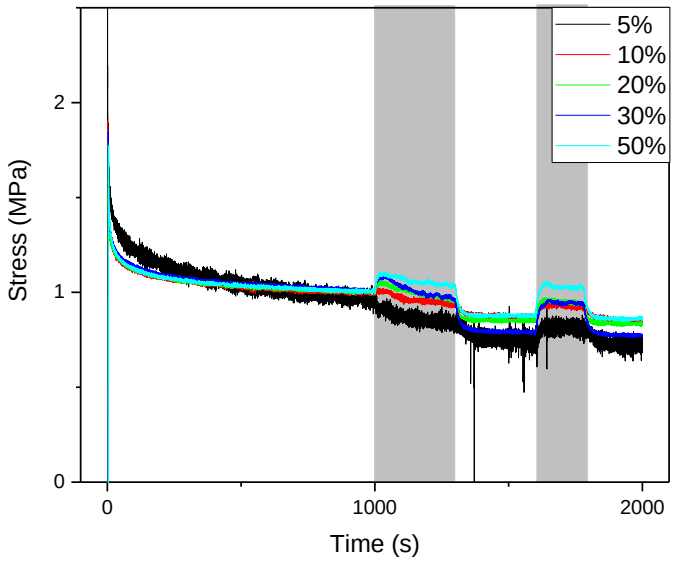

Figure 14: Normalized stress response of cycle 2

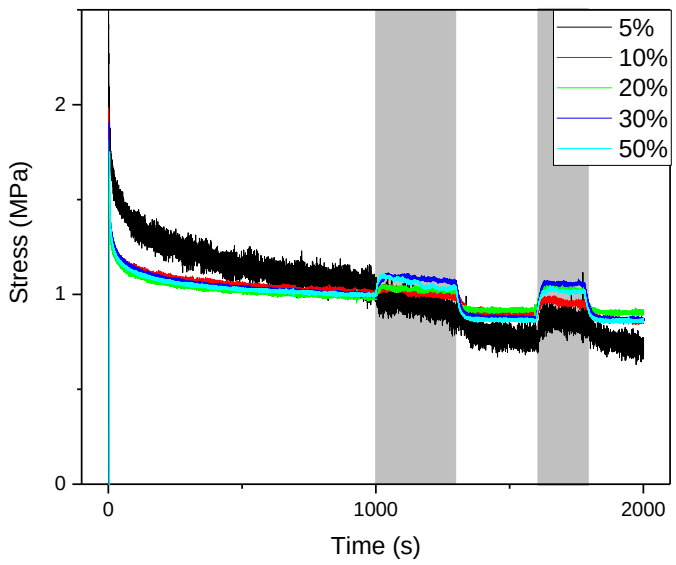

Figure 15: Normalized stress response of cycle 3

Understanding the effects of parameters of light such as intensity, frequency, and polarity on the composite is pertinent to gauge the effects of light on the actuation phenomenon. This study is mainly focused on effects of the intensity of the light on the composites. It was achieved by varying light intensity using neutral density filter (Thor Labs Inc.) between 14 and 97 mW/cm^2. The specimens were tested in the same way as described earlier by keeping the specimen under strain. Figure 16 depicts the stress-time graph of the performed tests.

The stress response for a light intensity of 14 mW/cm^2 was almost negligible with no noticeable irreversible response. Under the light intensity 30 mW/cm^2, the specimen produced a weak response, however, more pronounced than 14 mW/cm^2. The irreversible is weak, but distinguishable. The reversible stress response could be distinguished from

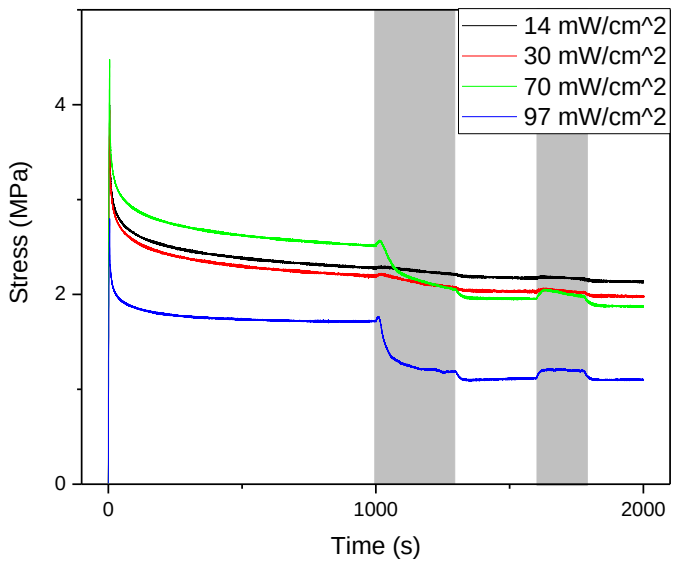

Figure 16: Stress responses at various light intensities

the normal stress response. For 70 mW/cm^2 the stress response was more pronounced than it was for 14 and 30 mW/cm^2 light intensities. Irreversible stress response showed a significant drop in stress and the peak value for reversible stress response was also higher. The irreversible and reversible stress responses showed the largest drop and highest peak stress response for 97 mW/cm^2 amongst the tested light intensities. From the graphs, an obvious trend of increasing peak value for reversible and larger drop for irreversible stress response with increased light intensities. For each attempt, as the light intensity was increased, CNT produced more thermal energy. Consequently, higher temperature melted more crystalline domains leading to increased stress response. To verify the assumption, two tests were conducted. For the first test, the specimen was irradiated with the gradually increasing intensity of light at fixed intervals from 14 to 97 mW/cm^2. In the second test, the light intensity was reduced from 97 to 14 mW/cm^2.

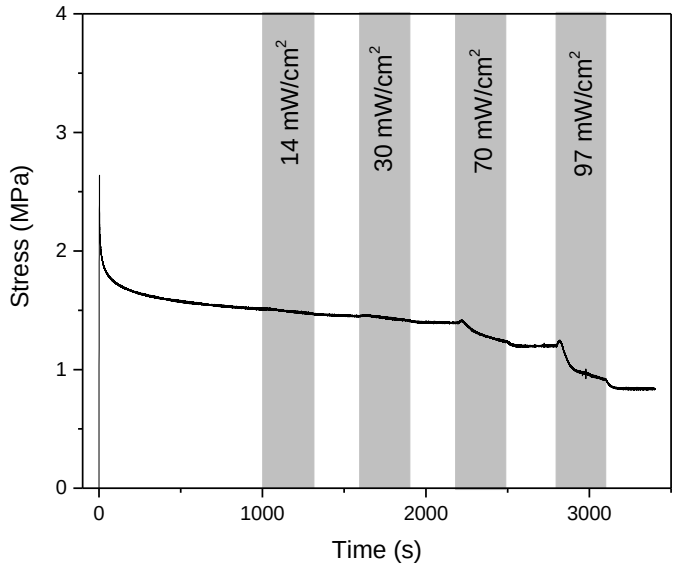

Figure 17: Stress response as the light intensity is increased from 14 to 97 mW/cm^2

Figure 17 depicts the stress-time graphs of the tests conducted. The specimen was stretched and held at 50% uniaxial tensile strain and allowed to relax into a quasi-equilibrium state till t = 1000s. Specimen was irradiated with light for 300s and the light source was switched off for the subsequent 300s. Light intensities were increased in an increasing order for the successive irradiations. The interval of irradiation of light is marked in grey in the graph. When the light intensity was increased from 14 to 97 mW/cm^2, the irreversible stress response steadily increased with subsequent higher light intensities. With the light intensity of 14 mW/cm^2, only a few of the crystalline domains could be melted. Thus, the irreversible response was very low. With higher light intensities of 30, 70 and 97 mW/cm^2, higher temperatures were attained, melting more crystalline domain than its preceding intensities leading to larger drops in irreversible stress response. The largest drop was observed for 97 mW/cm^2.

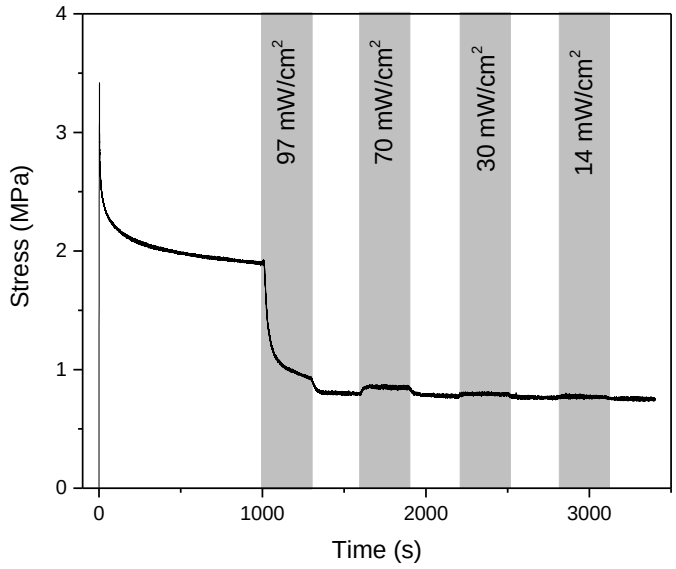

Figure 18: Stress response as the light intensity is decreased from 97 to 14 mW/cm^2

The second test was conducted in a similar manner, by modulating light intensity from 97 to 14 mW/cm^2 as shown in figure 18. The largest irreversible response was obtained for 97 mW/cm^2 and no further response was obtained for the subsequent lower intensities. The responses for lower intensities were similar to reversible responses of corresponding light intensities. This phenomenon could be explained as, when light with intensity 97 mW/cm^2 was irradiated on the specimen, the temperature increase in the specimen was high enough to melt a large portion of the crystalline domain which recrystallized upon removal of light. In the successive irradiations, the temperature increase was not sufficient to cause a further irreversible response, but sufficient to replicate reversible responses.

The results support the possibility of crystalline domains being the cause for actuation response in RET-MWCNT composite systems. To detect the change in the

number density of crystalline domains tests were conducted wherein uniaxial tensile strain was loaded to a predetermined value. The specimen was loaded from the strain-free state at a fixed strain rate of 10^{-4}/s. The specimen was irradiated the specimen with a specific light intensity throughout the test. Figure 19 shows the stress-stretch graph of RET-CNT specimens at different light intensities. With RET-CNT composite exhibiting elastomeric properties, the Neo-Hookean model was adopted to relate stress and strain as:

$$\sigma = G\left(\lambda^2 - \frac{1}{\lambda}\right) \tag{3}$$

where σ is the stress, λ is the stretch, formulated as 1+ε and G is the shear modulus. G, the slope of the graph is linearly proportional to the number density of crystalline domain, N, as:

$$G = Nk_BT \tag{4}$$

where k_B is the Boltzmann constant (1.38 x 10^{-23} JK^{-1}) and T is the temperature. Shear Modulus was calculated as the slope of figure 19 and plotted against strain ε in figure 20 for different light intensities. The reducing trend of shear modulus with the increasing uniaxial tensile strain shows that the nanocomposite softens upon stretching. Light intensity further modulates the softening of nanocomposite as seen in the graph. With the increase in light intensity, an increased rate of reduction of shear modulus with respect to tensile strain was observed. Since G is directly proportional to N from equation 4, number density of crystalline domain reduces with light intensity. The phenomenon observed reinforces the hypothesis of softening of nanocomposite by melting of crystalline domains.

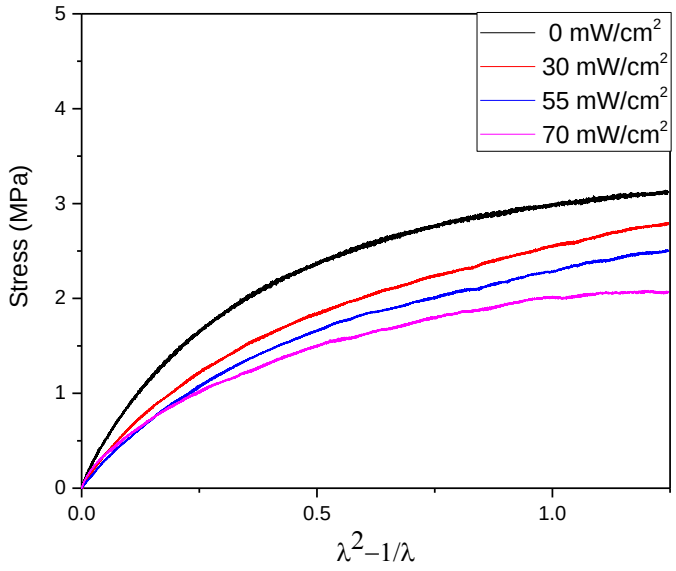

Figure 19: Stress and stretch relation of RET-MCNT composite in uniaxial tensile test with strain rate at 10^{-4}/s

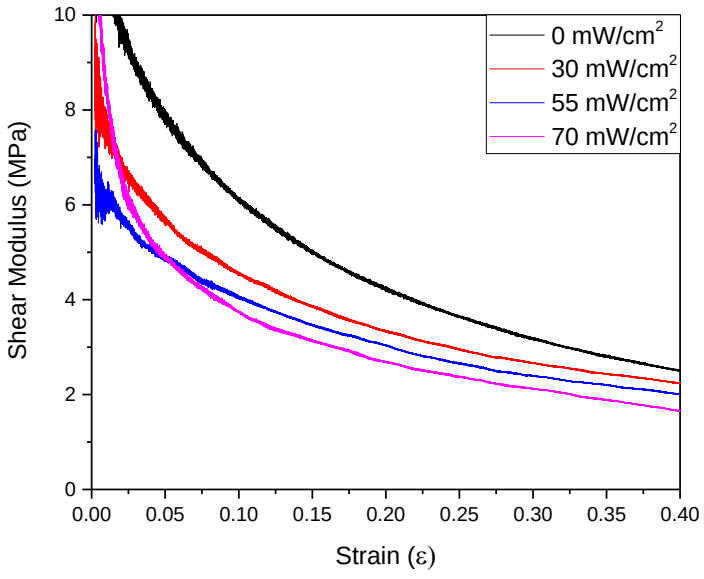

Figure 20: Shear modulus G under different light intensities with respect to strain ε

Chapter 4, in part, has been submitted for publication of the material as it may appear in. “Light induced reversible and irreversible deformation in nanotube-polymer composites”, 2017, X Liang, Z Zhang, A Sathisha, S Cai, P Bandaru, Polymer, 2017. The thesis author was the co-author of this paper.

5. PROPOSED MECHANISM

This section focusses on providing a detailed description of the proposed mechanism of photomechanical actuation in RET-CNT composite specifically, in the context of conducted tests. Structurally, RET is composed of three monomers, each serving different purposes. The epoxide group latches itself onto the CNT dispersed in the composite and serves as an anchor. The butyl group, with relatively low glass transition temperature serves as the soft segment in the composite. The ethylene group forms the physical crosslinks in the composite by forming crystalline domains.

The polymer chains in between crystalline domains are stretched when the composite is subjected to tensile strain on the composite. When the light is irradiated on the composite, the dispersed CNTs convert the light energy into thermal energy and melt the crystalline domains. The melting of crystalline domains results in the partial release of stress from the polymer chains connecting the crystalline domains, leading to the reported irreversible stress response. When the light source is switched off, the resulting decrease in matrix temperature would facilitate the recrystallization of melted crystalline domains. However, the released stress from the polymer chain would not reaccumulate. In the following light irradiations, the crystalline domains would melt and recrystallize upon light irradiations in a similar manner, but lead to the reported reversible stress response instead. During the ensuing reversible stress response, there would be no further partial stress release from the polymer chains under the same or lesser light intensity. However, if the irradiated light intensity is to be increased, a partial stress release from the polymer chains could be observed leading to another irreversible stress response. Figure 21 shows the representation of the mechanism.

Comparing the results with PDMS-CNT composite, the noticeable absence of irreversible stress response could be attributed to structural nuances between the PDMS and RET. The lack of ethylene segments to form physical crosslinks and epoxide group to anchor onto the CNTs could be suspected for the lack of irreversible stress response in the PDMS system, effectively results in a response observed in figure 7.

Chapter 5, in part, has been submitted for publication of the material as it may appear in. “Light induced reversible and irreversible deformation in nanotube-polymer composites”, 2017, X Liang, Z Zhang, A Sathisha, S Cai, P Bandaru, Polymer, 2017. The thesis author was the co-author of this paper.

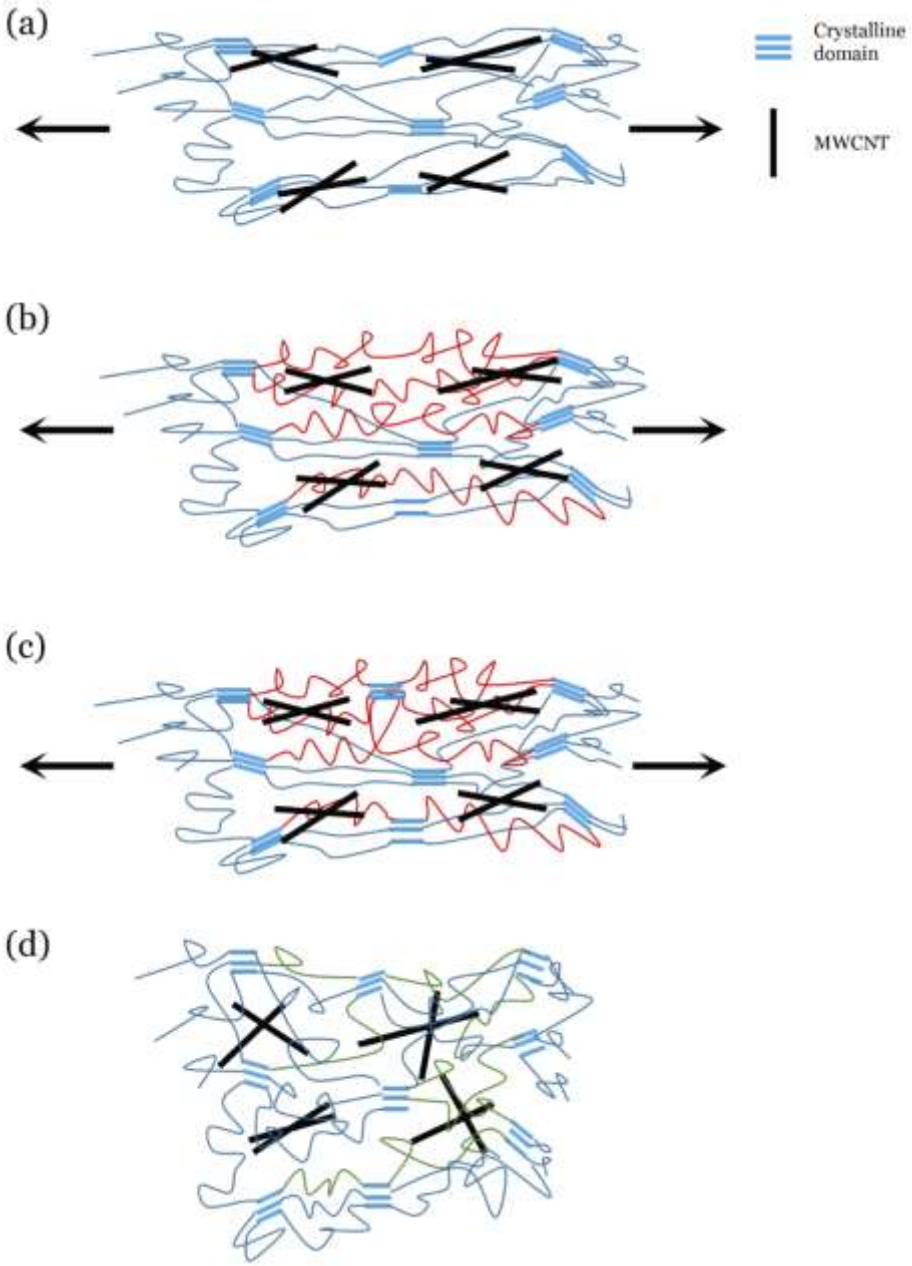

Figure 21: Mesoscopic model for the photo-response in RET-MWCNT composite. (a) Composite subjected to pre-strain. (b) Light irradiation induces melting of crystalline domains. (c) Crystalline domains reform upon switching off light source, reconnecting the relaxed polymer chains. (d) Plastic deformation exists in a freestanding composite

6. CONCLUSION

This study explored the photomechanical actuation in RET-CNT composite in conjunction with PDMS-CNT composite. The effects of parameters such as light intensity and uniaxial tensile strain were individually examined in detail through stress response measurements. Dual stress responses encompassing irreversible and reversible stress response observed during the tests were studied.

The absence of irreversible response in PDMS-CNT composite posited the assumption that the heat due to CNT transformed crystalline domains of RET to amorphous domains. Based on the results obtained, a microscopic model based on the melting of crystalline domains was proposed to explain the actuation process in the composite.

The dissertation concludes that the interface between CNT and the polymer plays a major role in the process. This study ends with the hope that it would provide motivation for deeper investigation of the role of interfaces.

7. REFERENCES

[1] S. Iijima, “Helical microtubules of graphitic carbon,” *Nature*, vol. 354, no. 6348, pp. 56–58, 1991.

[2] N. Behabtu, C. C. Young, D. E. Tsentalovich, O. Kleinerman, X. Wang, A. W. K. Ma, E. A. Bengio, R. F. ter Waarbeek, J. J. de Jong, R. E. Hoogerwerf, S. B. Fairchild, J. B. Ferguson, B. Maruyama, J. Kono, Y. Talmon, Y. Cohen, M. J. Otto, and M. Pasquali, “Strong, light, multifunctional fibers of carbon nanotubes with ultrahigh conductivity.,” *Science (80-.).*, vol. 339, no. 6116, pp. 182–6, 2013.

[3] R. H. Baughman, A. a Zakhidov, and W. a de Heer, “Carbon nanotubes --- the route toward applications,” *Science (80-.).*, vol. 297, no. 5582, pp. 787–92, 2002.

[4] M. F. L. De Volder, S. H. Tawfick, R. H. Baughman, and A. J. Hart, “Carbon Nanotubes: Present and Future Commercial Applications,” *Sci. (New York, NY)*, vol. 339, no. 6119, pp. 535–539, 2013.

[5] A. Maziz, A. Concas, A. Khaldi, J. Stålhand, N.-K. Persson, and E. W. H. Jager, “Knitting and weaving artificial muscles,” *Sci. Adv.*, vol. 3, no. 1, pp. 1–12, 2017.

[6] R. H. Baughman, “Playing Nature ’s Game with Artificial Muscles,” *Science (80-.).*, vol. 308, no. 5718, pp. 63–65, 2005.

[7] S. V. Ahir and E. M. Terentjev, “Fast relaxation of carbon nanotubes in polymer composite actuators,” *Phys. Rev. Lett.*, vol. 96, no. 13, 2006.

[8] R. H. Baughman, C. Cui, A. A. Zakhidov, Z. Iqbal, J. N. Barisci, G. M. Spinks, G. G. Wallace, A. Mazzoldi, D. De De Rossi D, A. G. Rinzler, O. Jaschinski, S. Roth, and M. Kertesz, “Carbon nanotube actuators,” *Science*, vol. 284, no. 5418, pp. 1340–4, 1999.

[9] R. Vaia, “Nanocomposites: remote-controlled actuators.,” *Nat. Mater.*, vol. 4, pp. 429–430, 2005.

[10] E. F. Crawley and J. De Luis, “Use of piezoelectric actuators as elements of intelligent structures,” *Aiaa J.*, vol. 25, no. 10, pp. 1373–1385, 1987.

[11] S. Frank, P. Poncharal, Z. L. Wang, and W. A. de Heer, “Carbon nanotube quantum resistors,” *Sci. (Washington, D. C.)*, vol. 280, no. 5370, pp. 1744–1746, 1998.

[12] S. Iijima and T. Ichihashi, “Single-shell carbon nanotubes of 1-nm diameter,” *Nature*, vol. 363, pp. 603–605, 1993.

[13] D. S. Bethune, C. H. Klang, M. S. de Vries, G. Gorman, R. Savoy, J. Vazquez, and R. Beyers, “Cobalt-catalysed growth of carbon nanotubes with single-atomic-layer walls,” *Nature*, vol. 363, no. 6430, pp. 605–607, 1993.

[14] Y. Lin, F. Lu, Y. Tu, and Z. Ren, “Glucose Biosensors Based on Carbon Nanotube Nanoelectrode Ensembles,” *Nano Lett.*, vol. 4, no. 2, pp. 191–195, 2004.

[15] D. N. Futaba, K. Hata, T. Yamada, T. Hiraoka, Y. Hayamizu, Y. Kakudate, O. Tanaike, H. Hatori, M. Yumura, and S. Iijima, “Shape-engineerable and highly densely packed single-walled carbon nanotubes and their application as super-capacitor electrodes.,” *Nat. Mater.*, vol. 5, no. December, pp. 987–994, 2006.

[16] M. S. Dresselhaus, G. Dresselhaus, and R. Saito, “Physics of carbon nanotubes,” *Carbon N. Y.*, vol. 33, no. 7, pp. 883–891, 1995.

[17] G. Overney, W. Zhong, and D. Tomanek, “Structural Rigidity and Low-Frequency Vibrational-Modes of Long Carbon Tubules,” *Zeitschrift Fur Phys. D-Atoms Mol. Clust.*, vol. 27, no. 1, pp. 93–96, 1993.

[18] J. N. Coleman, U. Khan, W. J. Blau, and Y. K. Gun’ko, “Small but strong: A review of the mechanical properties of carbon nanotube-polymer composites,” *Carbon N. Y.*, vol. 44, no. 9, pp. 1624–1652, 2006.

[19] E. W. Wong, P. E. Sheehan, and C. M. Lieber, “Nanobeam Mechanics: Elasticity, Strength, and Toughness of Nanorods and Nanotubes,” *Science (80-.).*, vol. 277, no. 5334, pp. 1971–1975, 1997.

[20] M. Yu, “Strength and Breaking Mechanism of Multiwalled Carbon Nanotubes Under Tensile Load,” *Science (80-.).*, vol. 287, no. 5453, pp. 637–640, 2000.

[21] Z. Han and A. Fina, “Thermal conductivity of carbon nanotubes and their polymer nanocomposites: A review,” *Prog. Polym. Sci.*, vol. 36, no. 7, pp. 914–944, 2011.

[22] D. Tasis, N. Tagmatarchis, A. Bianco, and M. Prato, “Chemistry of carbon nanotubes,” *Chem. Rev.*, vol. 106, no. 3, pp. 1105–1136, 2006.

[23] S. H. Park and P. R. Bandaru, “Improved mechanical properties of carbon nanotube/polymer composites through the use of carboxyl-epoxide functional group linkages,” *Polymer (Guildf).*, vol. 51, no. 22, pp. 5071–5077, 2010.

[24] J. Hilding, E. a. Grulke, Z. George Zhang, and F. Lockwood, “Dispersion of Carbon Nanotubes in Liquids,” *J. Dispers. Sci. Technol.*, vol. 24, no. 1, pp. 1–41, 2007.

[25] S. V. Ahir, Y. Y. Huang, and E. M. Terentjev, “Polymers with aligned carbon nanotubes: Active composite materials,” *Polymer (Guildf).*, vol. 49, no. 18, pp. 3841–3854, 2008.

[26] H. Yazdani, B. E. Smith, and K. Hatami, “Multi-walled carbon nanotube-filled polyvinyl chloride composites: Influence of processing method on dispersion quality, electrical conductivity and mechanical properties,” *Compos. Part A Appl. Sci. Manuf.*, vol. 82, pp. 65–77, 2016.

[27] P. C. Ma, N. A. Siddiqui, G. Marom, and J. K. Kim, “Dispersion and functionalization of carbon nanotubes for polymer-based nanocomposites: A review,” *Compos. Part*

A Appl. Sci. Manuf., vol. 41, no. 10, pp. 1345–1367, 2010.

[28] S. V Ahir and E. M. Terentjev, “Photomechanical actuation in polymer-nanotube composites.,” *Nat. Mater.*, vol. 4, no. 6, pp. 491–5, 2005.

[29] C. T. Love and V. M. Karbhari, “Filled reactive ethylene terpolymer primers for cathodic disbondment mitigation,” *J. Appl. Polym. Sci.*, vol. 110, no. 3, pp. 1531–1544, 2008.